Mach Number and Static Pressure Determination Based on Oblique Shock Theory

by Dr. F. W. Ross

Aeronautical Research Center
University of Michigan

Project MX-794
(USAF Contract W33-038-ac-14222)

UMM-33 August 1, 1949

TABLE OF CONTENTS

LIST OF FIGURES

INTRODUCTION

A new method has been developed for obtaining important supersonic wind tunnel calibration constants. This method makes possible better correlation between theoretical studies and experimental data than has been possible in the past.

Until recently the correlation between supersonic theory and experiment for currently available data has been considered generally satisfactory. With the improvements of flow conditions in the newer wind tunnels now under development, however, the scatter of data has been reduced sufficiently so that discrepancies between theory and experiment have become evident.

The general status of experimental scatter and correlation of older data are illustrated by the examples shown in figure 1. (See also refs. 1, 2,3,4). Data obtained from more recently developed wind tunnels have shown considerable improvement. In particular, the data from the University of Michigan supersonic wind tunnel have shown much less scatter. While the correlation is better than before, the more consistent data have made it possible to observe a definite discrepancy between theory and the data. In figures 2, 3, and 4 the data from a wedge, a cone, and a cone-cylinder are compared to theory using previous methods of tunnel calibration. The experimental scatter is notably less. It is observed, however, that all the experimentally determined coefficients appear to be definitely higher than the theoretically predicted values (Refs. 5 and 6).

This discrepancy has been removed by the development of a new method for wind tunnel calibration. The method requires no assumptions about the duct losses upstream of the point under consideration, nor about the value of the stagnation pressure, p_o. All quantities are determined in terms of conditions at the point under consideration only. The method also removes uncertainties of determination of static pressure by static probe method. An accurate three-way check of the results is included as part of the procedure.

The data were obtained from the University of Michigan supersonic wind tunnel located at Willow Run. This tunnel is of the blow-down type with the high pressure side essentially at atmospheric pressure.

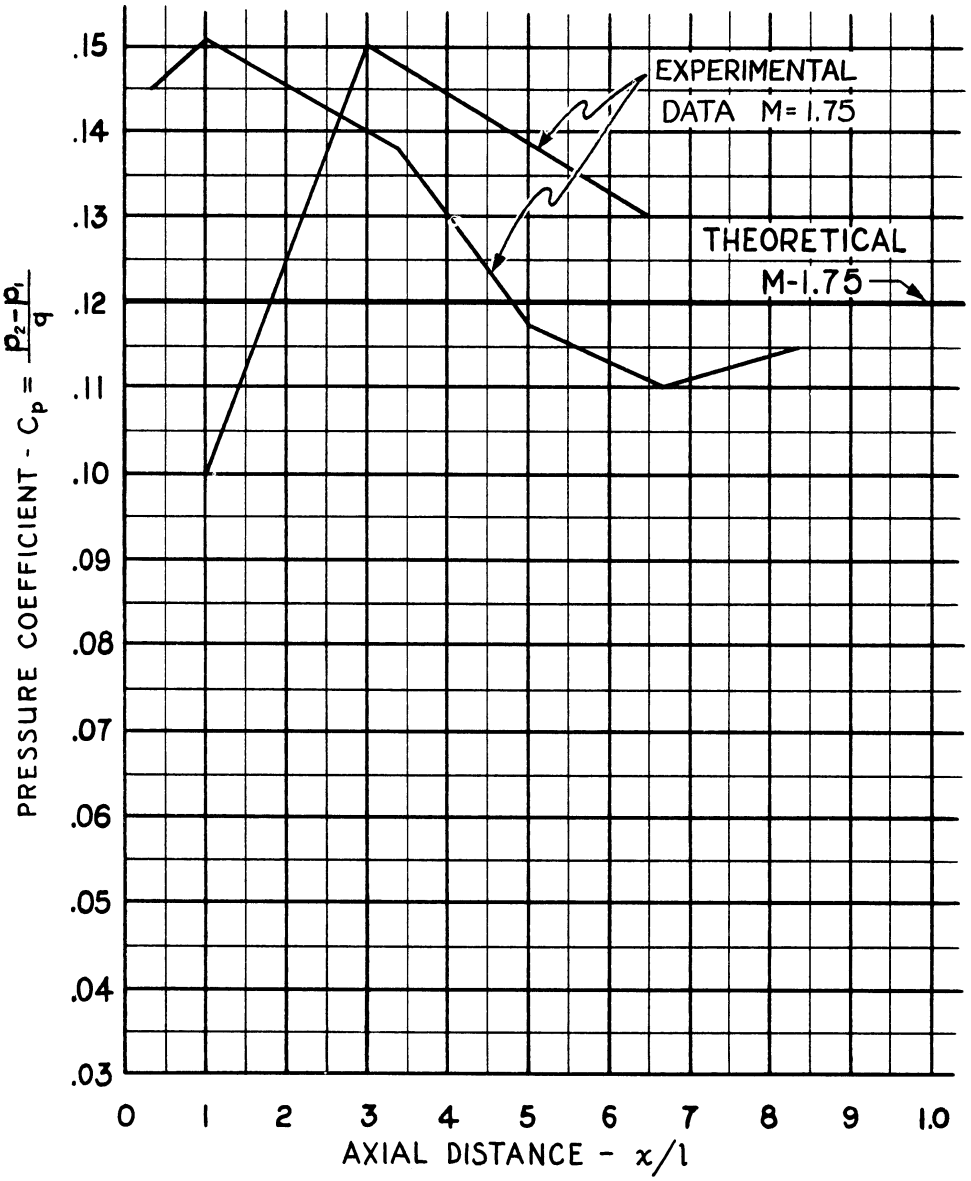

FIG. 1 – CORRELATION BETWEEN THEORY AND EXPERIMENT CHARACTERISTIC OF OLDER DATA (REF. 1 & 2) FOR 20° CONE

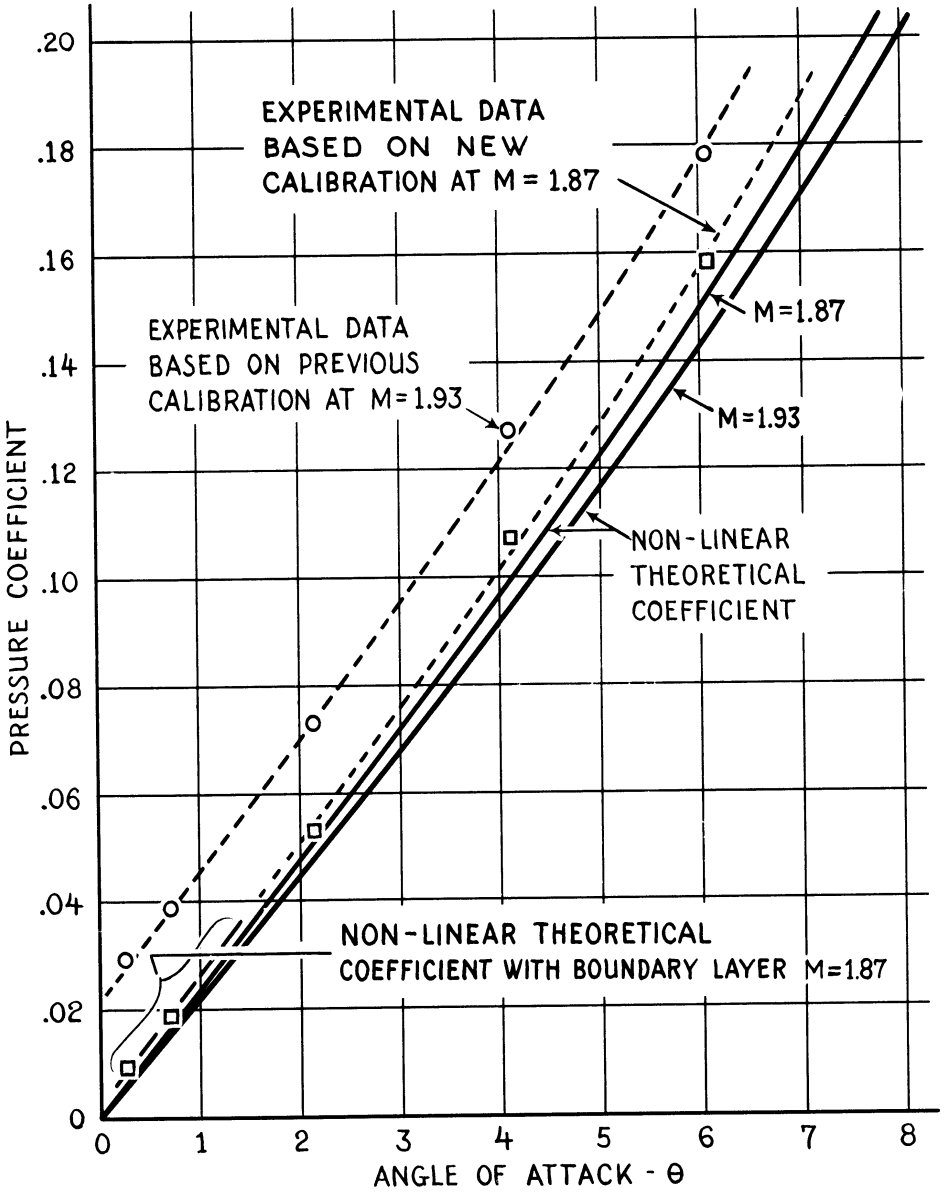

FIG. 2 – WEDGE PRESSURE COEFFICIENT

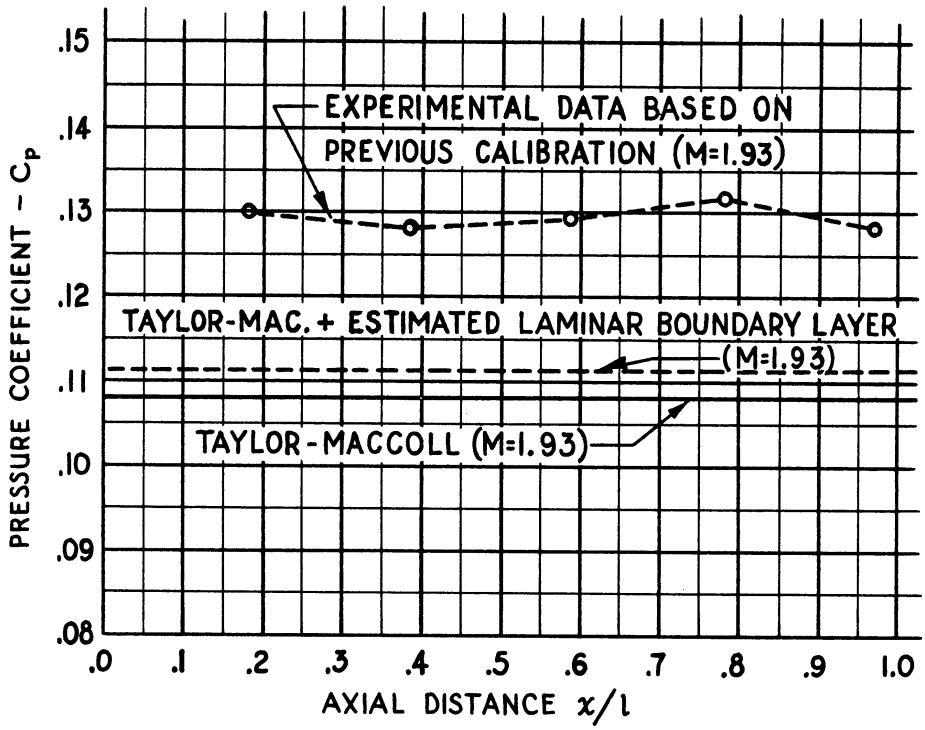

FIG. 3 – PRESSURE COEFFICIENT VS AXIAL POSITION FOR 20° CONE, $\alpha = 0$

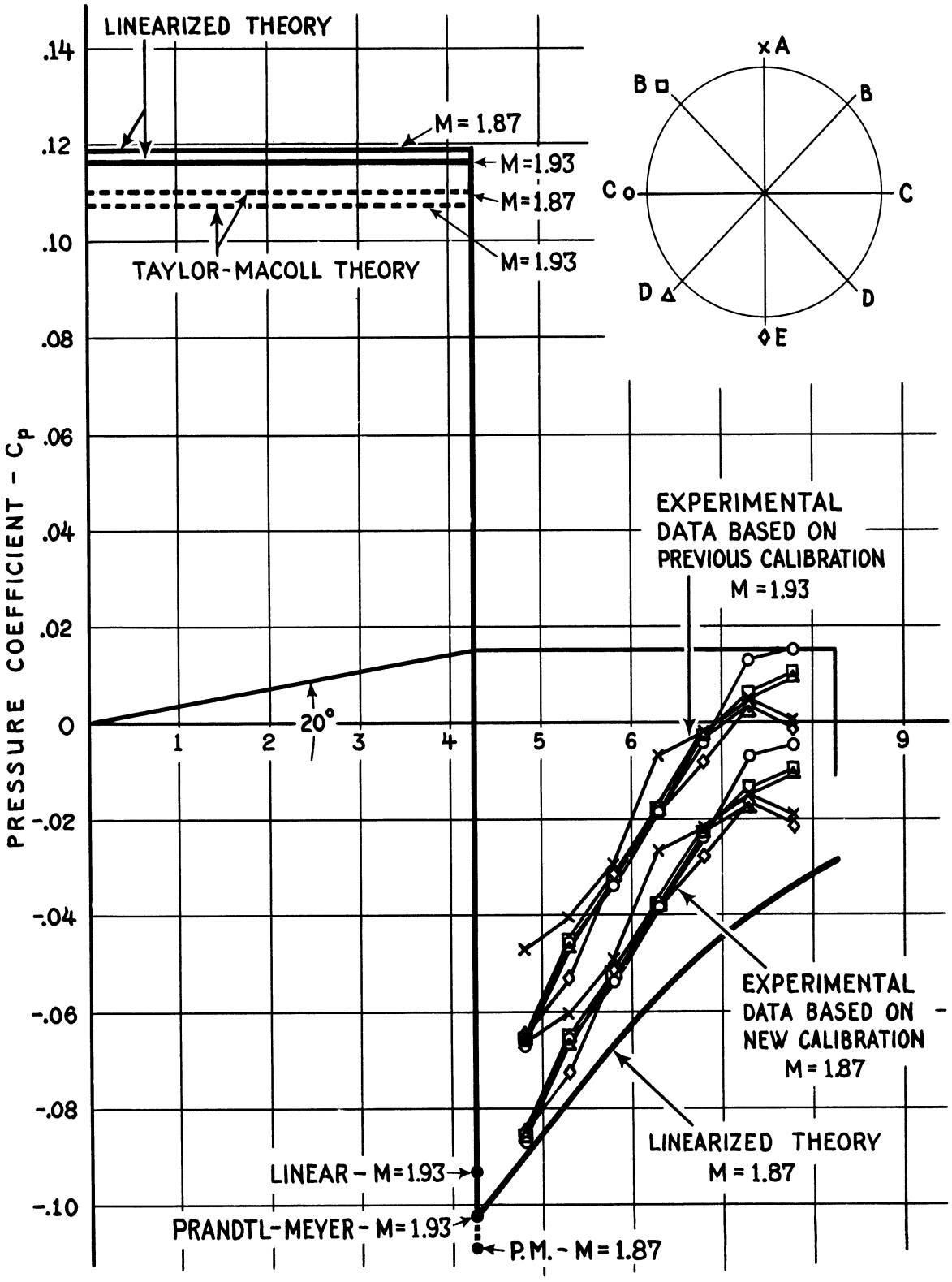

FIG. 4 – PRESSURE COEFFICIENT VS AXIAL POSITION FOR CONE-CYLINDER MODEL, $\alpha = 0$

THEORY OF THE METHOD

Conditions pertaining to the flow about a plane surface inclined to a supersonic stream may be described, through oblique shock wave theory, by the equations*

$$\frac{p_2}{p_1} = \frac{2\gamma}{\gamma+1} M_1^2 \sin^2\beta - \frac{\gamma-1}{\gamma+1} \tag{1}$$

$$\frac{1}{M_1^2} = \sin^2\beta - \frac{\gamma+1}{2} \frac{\sin\beta \sin\theta}{\cos(\beta-\theta)} \tag{2}$$

$$p_2 - p_1 = \rho_1 u_1^2 \frac{\sin\beta \sin\theta}{\cos(\beta-\theta)} \tag{3}$$

$$q = \frac{\gamma}{2} p_1 M_1^2 \tag{4}$$

where p_1 = ambient static pressure

M_1 = ambient Mach number

β = shock wave angle

θ = angle of attack of one inclined surface of the wedge

γ = ratio of specific heats

p_2 = pressure on inclined surface

q = dynamic pressure

Using these relations (1) the Mach number, (2) the ambient static pressure, and (3) the dynamic pressure are determined from values of

*See, for example, Liepmann and Puckett, "Aerodynamics of a Compressible Fluid", Wiley, p. 57

p_2 and β obtained by setting the inclined surface of a wedge at various angles of attack. The details are discussed in the following sections. The angles are illustrated in figure 5. With this method the angle, θ, of the inclined surface need not be known exactly. It enters only as a parameter. The independent determination of dynamic pressure and pressure behind a normal shock wave provide accurate means of checking the values determined for p_1 and M_1.

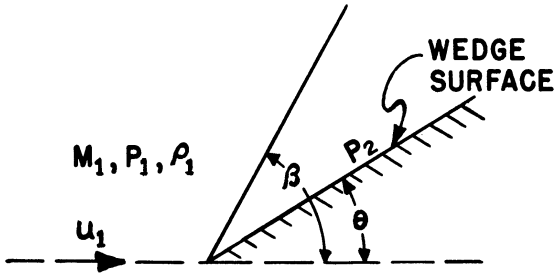

FIG. 5 – DIAGRAM SHOWING ANGLES

EXPERIMENTAL MODEL

A wedge with 16° included angle, as shown in figure 6, was used. The wedge had a chord of 1.375 inches and a span of 3 inches. This was adequate span to assure no interference from tip shocks for the angles of attack used in the tests. Three pressure orifices were located along the center line of each side 1/2, 3/4, and one inch from the leading edge. Inasmuch as only one side of the wedge was essential to the tests especial care was used to obtain an accurately ground plane surface on one side of the wedge. This is the lower surface as shown in the Schlieren photographs. The leading edge radius was sharp, the radius being estimated as less than 0.0005 inch.

DETERMINATION OF MACH NUMBER AND SHOCK WAVE ANGLE

Accurate determination of shock wave and Mach wave angles is an important part of the method. This is accomplished by superimposing a wire grid as a background on the Schlieren photographs of the flow. Thus, any distortion caused by the flow, the optical system, or the photographic process can be detected within an error less than ±0.1°. The grid, shown in figure 7, is placed on the source side of the tunnel section, as shown in figure 8. The grid was composed of 0.020 inch music wire spaced 0.2 inch apart covering an array 10 inches square. The wires were held in a metal frame with spacings cut by an accurate milling machine. Photographs without flow, with flow, and with no model and with flow about several models indicated that accuracies of ±0.1° can be obtained for determination of angles. The grid also serves as a means of determining any deflections in the model or its support. Figure 9 is a Schlieren photograph taken through the grid with no model in the tunnel.

FIG. 6 — 16° WEDGE MODEL

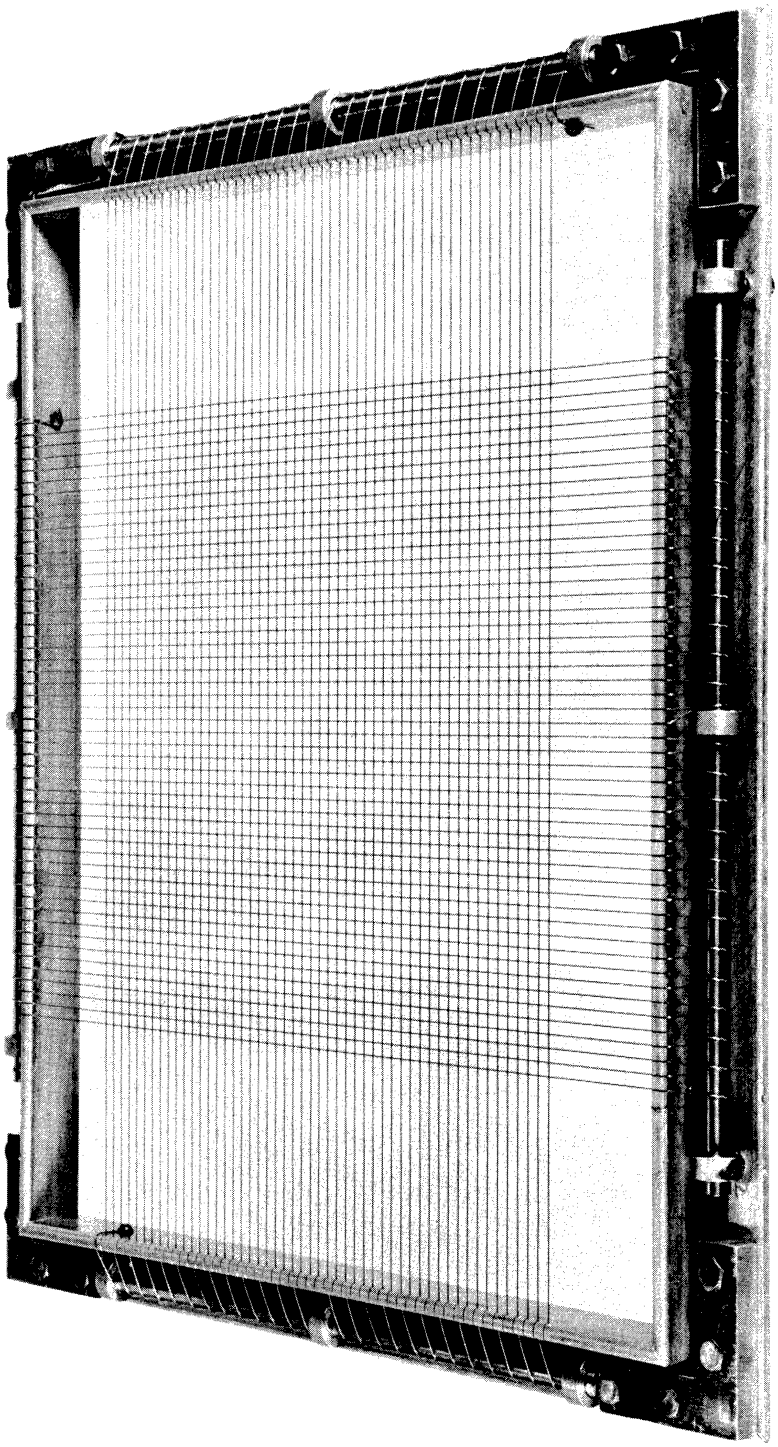

FIG. 7 – WIRE GRID

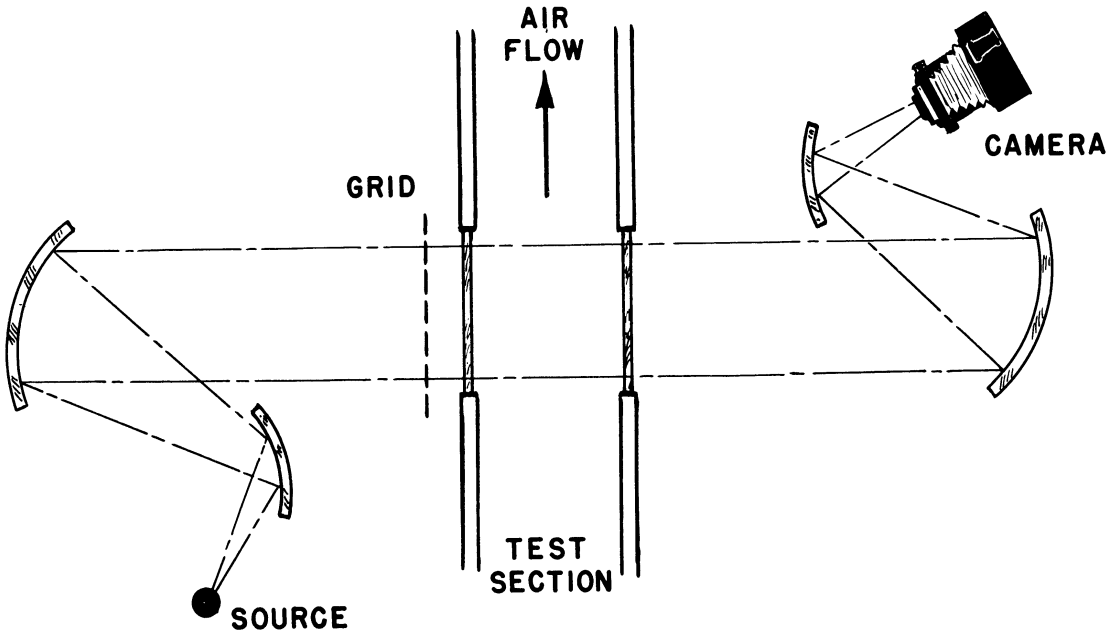

FIG. 8 – DIAGRAM SHOWING POSITION OF GRID

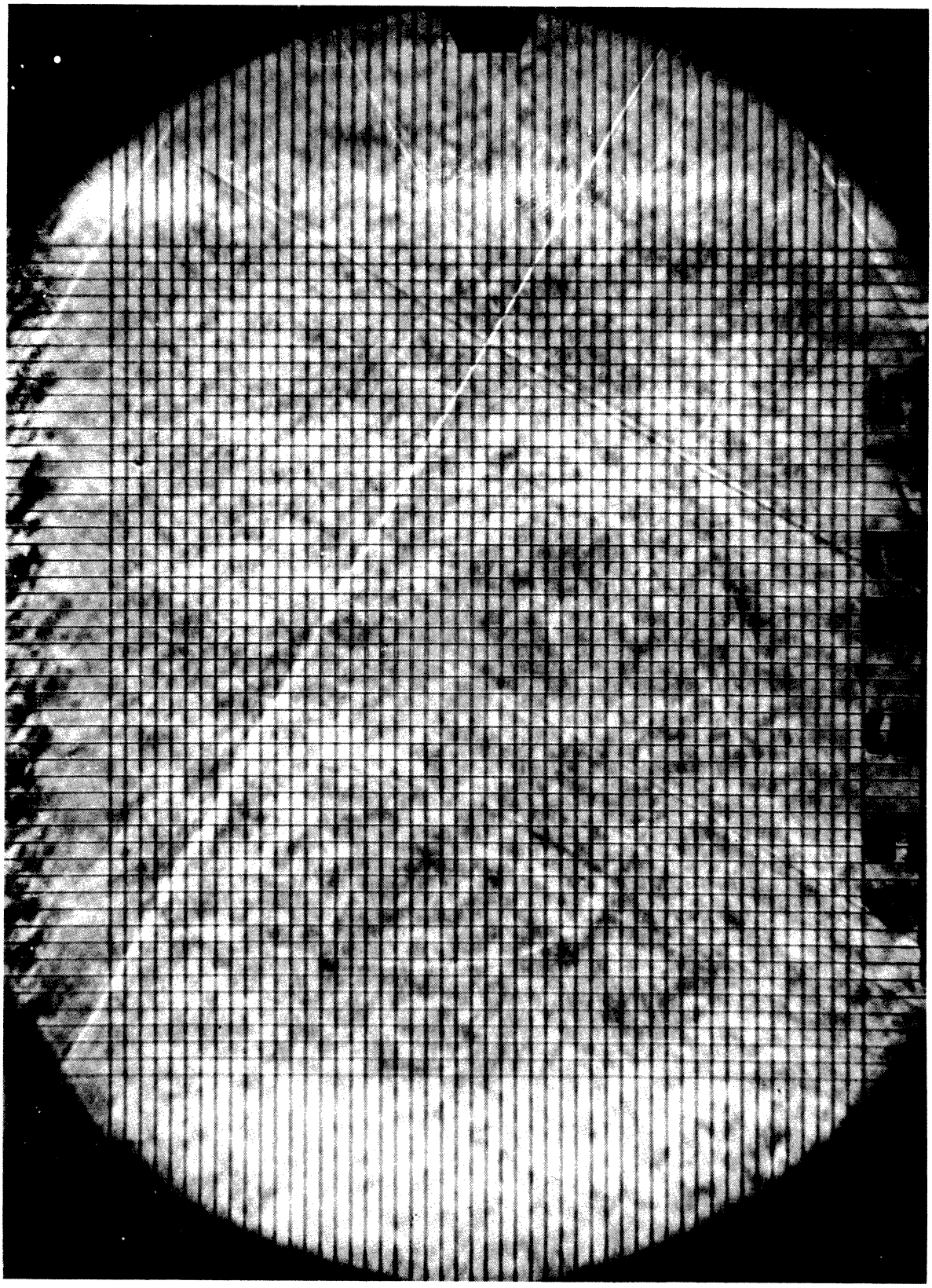

FIG. 9 – SCHLIEREN PHOTOGRAPH, WITH NO MODEL, AT M = 1.87, SHOWING WIRE GRID SUPERIMPOSED

DETERMINATION OF AMBIENT STATIC PRESSURE

The ambient static pressure, p_1 , is determined through use of equations (2) and (3). In equation (3), when $\theta = 0$, $\sin\theta$ vanishes and the equation becomes $p_2 = p_1$ The ambient static pressure, p_1 , can be determined then by measuring the pressure, p_2 , on a wedge surface placed so that it is aligned in the direction of flow (thus making $\theta = 0$).

The experimental realization of the setting of $\theta = 0$ is difficult. Account must be taken of any inclination in flow, of the effective shift in θ because of the boundary layer, and of any deflection of the supporting members. The determination of these corrections at best is always approximate and the alignment of the surface at $\theta = 0$ is left open to question.

When $\theta = 0$ equation (2) reduces to $\frac{1}{M_1} = \sin\beta = \sin\alpha$ and the shock angle, β , becomes the Mach angle, α . With M_1 and γ constant equation (2) implicitly determines β as a function of θ . For positive values of θ the derivative, $\frac{\partial\beta}{\partial\theta}$, is positive and approaches a limiting value at $\theta = 0$

$$\left(\frac{\partial\beta}{\partial\theta}\right)_{\theta=+0} = \frac{\gamma+1}{4\cos^2\alpha}$$

Since α is always a definite positive angle then the derivative $\frac{\partial\beta}{\partial\theta}$ is always some definite positive value at $\theta = +0$.

For negative values of θ , a fan of Mach lines is given off at the leading edge of the wedge. These are described in terms of the Prandl-Meyer* expansion around a corner.

The first of these Mach lines is characteristic of the flow in the undisturbed stream and its angle remains constant for all negative values of θ . Therefore, with the understanding that the upstream Mach line only is considered then the slope

$$\left(\frac{\partial\beta}{\partial\theta}\right)_{\theta=-0} = 0$$

*See, for example, Sauer, R. "Introduction to Theoretical Gas Dynamics" Edwards, 1947, p. 84

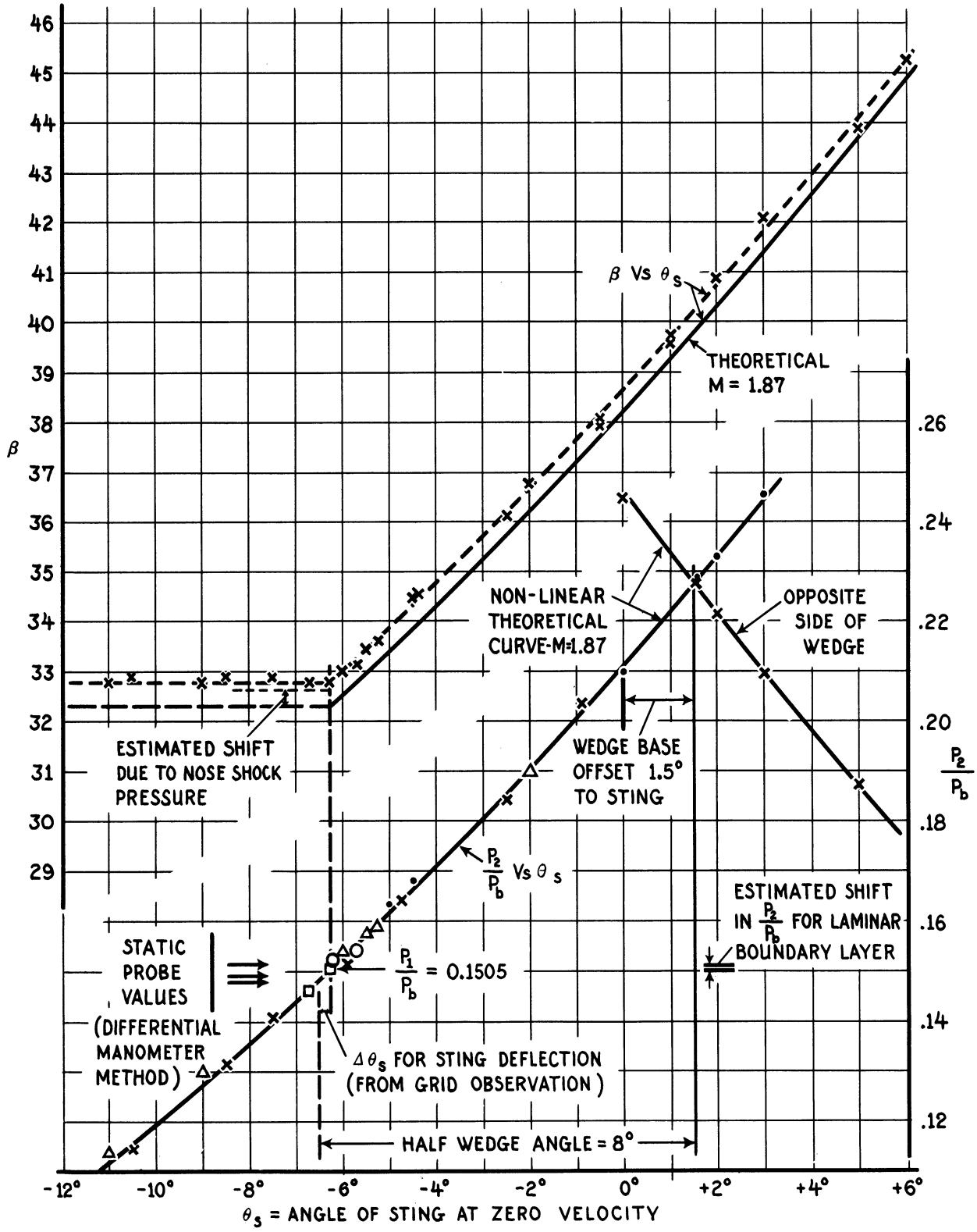

FIG. 10 – $\frac{P_2}{P_b}$ VS θ_s AND β VS θ_s FOR INCLINED WEDGE

Thus a discontinuity in $\frac{\partial\beta}{\partial\theta}$ exists at $\theta = 0$. If p_2 and β are determined experimentally in terms of some reference angle, $\theta_s = \theta + \theta_r$, as a parameter, a plot of $\beta = \beta(\theta_s)$ indicates accurately the value of $\theta_s = \theta_{s_1}$ for which $\theta = 0$. The corresponding value of p_2 at θ_{s_1} is then the ambient static pressure, p_1.

Plots of experimental data from several series of tests for $\beta = \beta(\theta_s)$ and $p_2 = p_2(\theta_s)$ are shown in figure 10. The sharpness of the discontinuity in $\beta = \beta(\theta)$ as predicted is noted.

The pressure data are given in terms of the ratio to barometric pressure, p_b. All quantities are either directly proportional to p_b or very nearly so. Hence, the effects of variation in p_b are essentially eliminated when the pressures are given as ratios to p_b. This is borne out by the agreement of data taken on different days when p_b was different.

Theoretically the Mach line given off from the leading edge of the wedge should be vanishingly weak for negative values of θ of the inclined surface. Actually, any model used will have some finite leading edge radius and consequently some greater disturbance is given off which produces a definite shock line.

A small static probe was used (Fig. 11) to measure the static pressure change across this shock line. The inclined surface was set approximately at the angle which corresponds to the discontinuity in $\beta = \beta(\theta)$. The pressures measured by this probe indicated that the pressure at positions greater than one-quarter inch aft of the shock line was the same as that ahead within 0.02" Hg. The gradations of density on figure 11 also indicate that the densities this far aft of the shock line have recovered closely to that of the density ahead. The pressure within the shock wave is higher by the order of 0.1" Hg. or a pressure ratio $p_2/p_1 = 1.023$. At a Mach number of 1.87 this would correspond to an increase in shock angle of 0.35° greater than the Mach angle. The difference in angle between the weak shock given off by the probe and the shock line given off by the knife edge is measured as 0.4 degree and, thus, agrees well with this value. The probe shock is too weak to be reproduced so it is dotted in figure 11 to indicate its position as determined from the original plate.

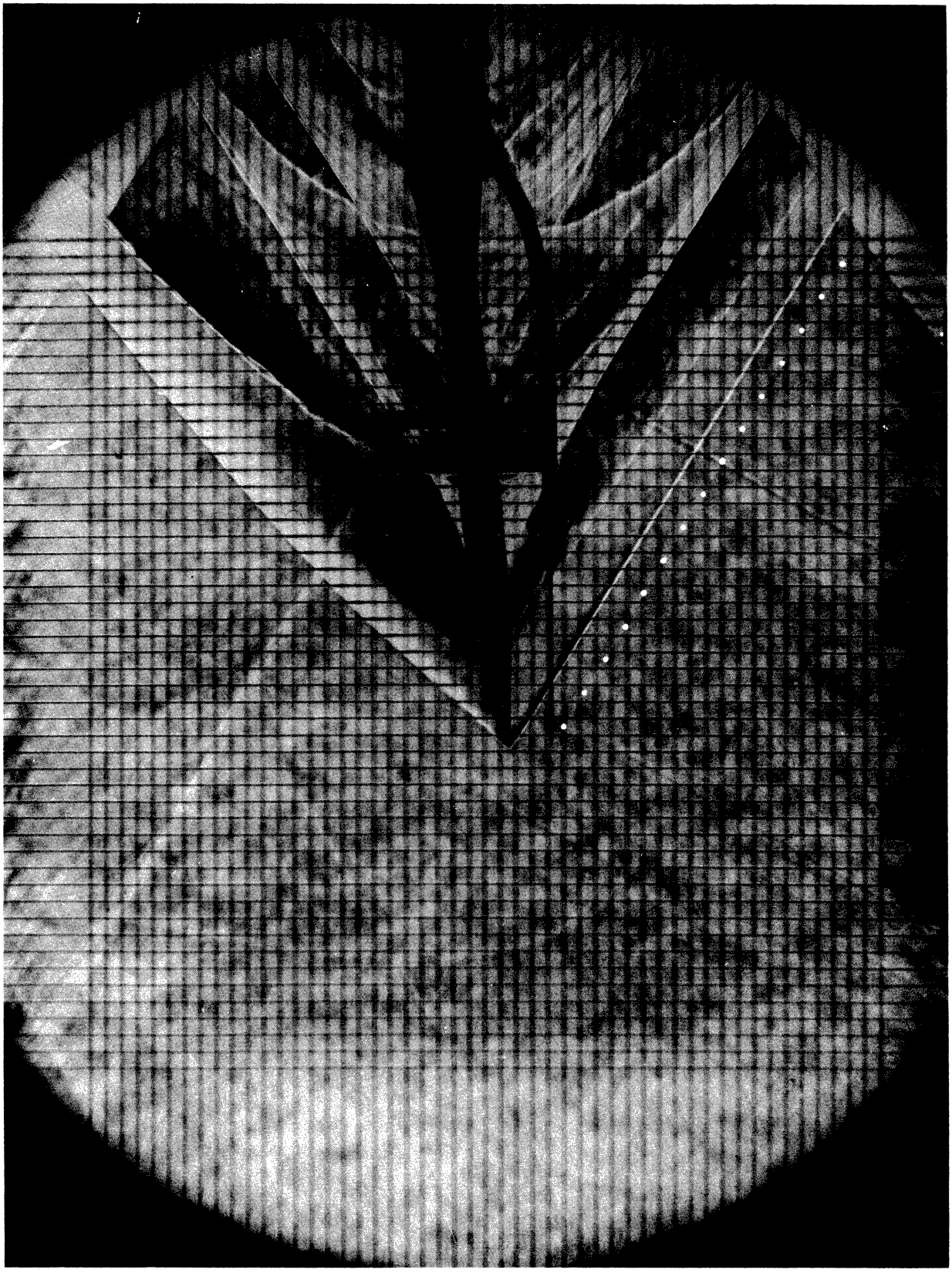

FIG. 11 - SCHLIEREN PHOTOGRAPH OF WEDGE AND STATIC PROBE

The effect of the finite nose radius was further studied by testing under the same conditions with an increased nose radius. The original nose radius ($r < 0.0005"$) introduces a shock line which has an angle shift of approximately 0.4^{o}. The effect of the nose radius is otherwise confined to the immediate vicinity of the nose. From figure 11 it is noted that the shock line is straight except within about 0.3" of the knife edge. Thus, by measuring angles and pressures well outside this region the effect of nose radius is eliminated. When the nose radius is increased about three times it is noted that the shock line is curved over a much larger region and extends several inches aft of the nose (see Fig. 12). Consequently, the conditions for which the theory obtains are not met. Data of these kind cannot be used. It is concluded then that the radius of the leading edge must be sharp enough so that the region of curved shock lines is small in comparison to the dimensions of the wedge and the orifice location. That such conditions were maintained in these tests is indicated in figure 11. Any curvature of the weak Mach line off the lower surface is confined to the region less than two squares (about 0.3") from the leading edge. This is well forward of the pressure orifices which were located 0.5 to 1.0 inch aft of the leading edge.

The shift in shock angle introduced by the nose pressure wave should shift the values of β nearly constant for negative values of θ. The shift should be decreasingly less as the pressure ratio increases for higher positive compressive angles θ. At $\theta_s = +4$, the shift should be about 0.6 of that at $\theta_s = -6$. Comparison of the theoretical curve with the experimental data on figure 10 indicates this. The effect on the discontinuity in the β vs. θ curve is negligible, however. And since the purpose of the curve is to locate the corresponding p_2 from the $p_2 = p_2(\theta)$ curve, then the effect of finite nose radius is avoided by maintaining the nose radius sufficiently small so that the curvature of the shock lines is confined to an unimportant region, as shown in figure 11, rather than as represented by figure 12. Attempts at determination of β from Fig. 12 have shown that the curvature and its effect on the pressure, p_2, make it impossible to determine the discontinuity in $\beta = \beta(\theta)$ with accuracy.

DETERMINATION OF DYNAMIC PRESSURE

The pressure ratio across an oblique shock wave is given by equation (1). Using the definition of dynamic pressure, q, given by

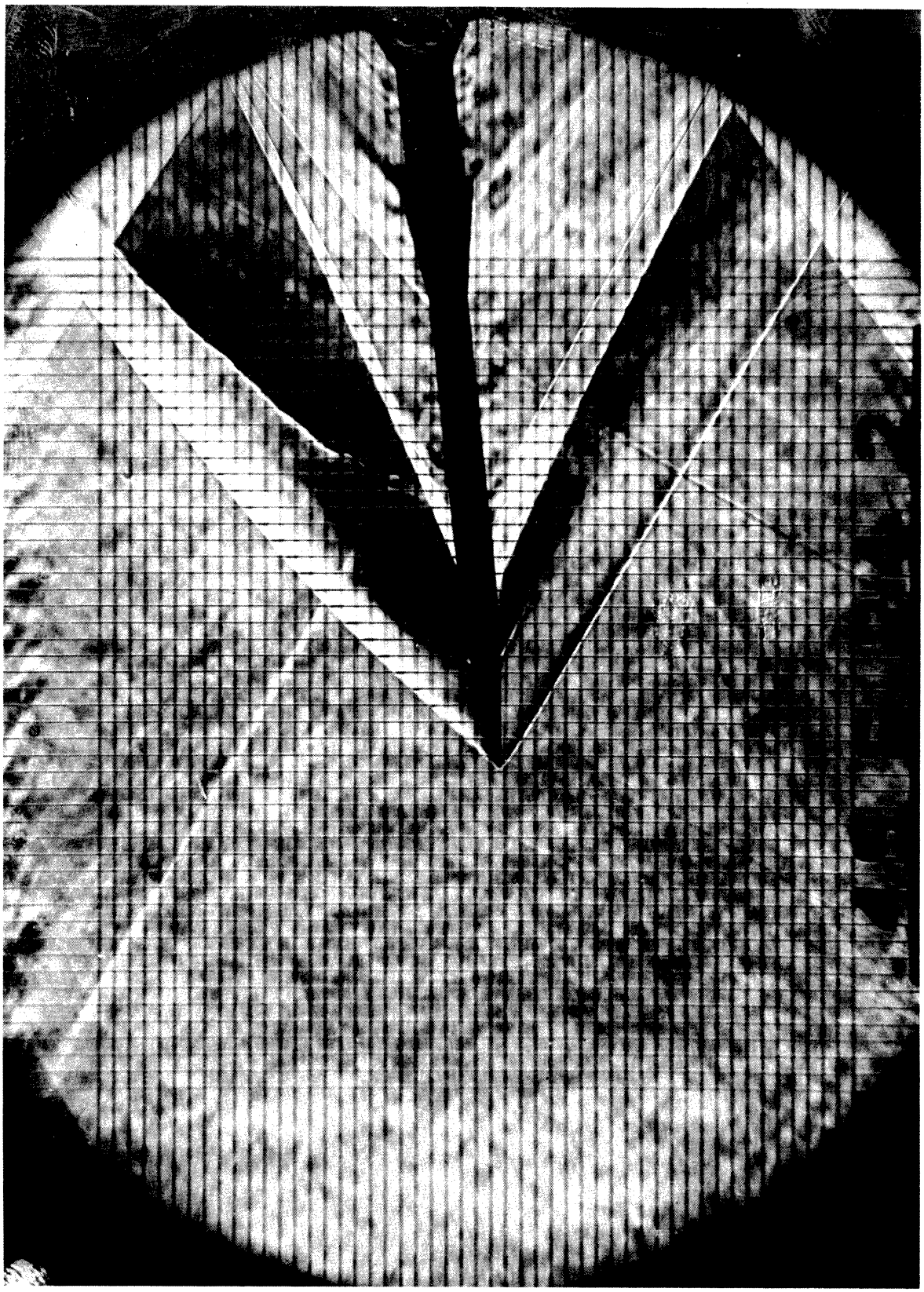

FIG. 12 - SCHLIEREN PHOTOGRAPH - LEADING EDGE RADIUS TOO LARGE

equation (4), equation (1) may be written as

$$p_2 = \frac{4}{\gamma + 1} q \sin^2 \beta - \frac{\gamma - 1}{\gamma + 1} p_1 \qquad (5)$$

For a given air stream, p_1 , M_1 , and γ are constant. Hence, by determining p_2 and β for various settings of θ the dynamic pressure, q, may be determined. Equation (5) is of the linear form $y = m x + b$ where $x = \sin^2 \beta$ and the slope m, is $\frac{4q}{\gamma + 1}$. Hence q may be readily determined from a plot of p_2 vs $\sin^2 \beta$. The two sets of data shown on figure 13 verify the linearity relationship and indicate the order of accuracy possible for determining the slope. Advantages of this method of determining the dynamic pressure are:

(a) The absolute value of p_2 need not be known. p_2 enters equation (5) in a manner so that the value of the reference is of no importance. It is only necessary to measure p_2 to the same reference during any particular determination. Thus, any additive shift in p_2 such as may be introduced by the small but finite nose of the knife edge will have no effect on q. The close fit to linearity as well as the agreement to the theoretically calculated $p_2 = p_2(\theta_s)$ curve on figure 10 are additional evidence that a shift, if any exists, must be additive within the accuracies attained here.

(b) The angle of setting of the wedge surface need not be known. p_2 is measured at a given reference setting of θ_s at the same time the Schlieren is taken. Hence, any deflection in the model sting, any effective shift in θ because of boundary layer build up, or inaccuracy in the θ setting, all such items have no effect on the results.

(c) The absolute value of β need not be known precisely. An error of 0.2 degree in β introduces an error less than 0.1% in dynamic pressure in the range considered. The absolute values of β are well within 0.2 degree.

Equation (5) may be written (as discussed previously)

$$\frac{p_2}{p_b} = \frac{4}{\gamma + 1} \left(\frac{q}{p_b}\right) \sin^2 \beta - \frac{\gamma - 1}{\gamma + 1} \left(\frac{p_1}{p_b}\right) \qquad (6)$$

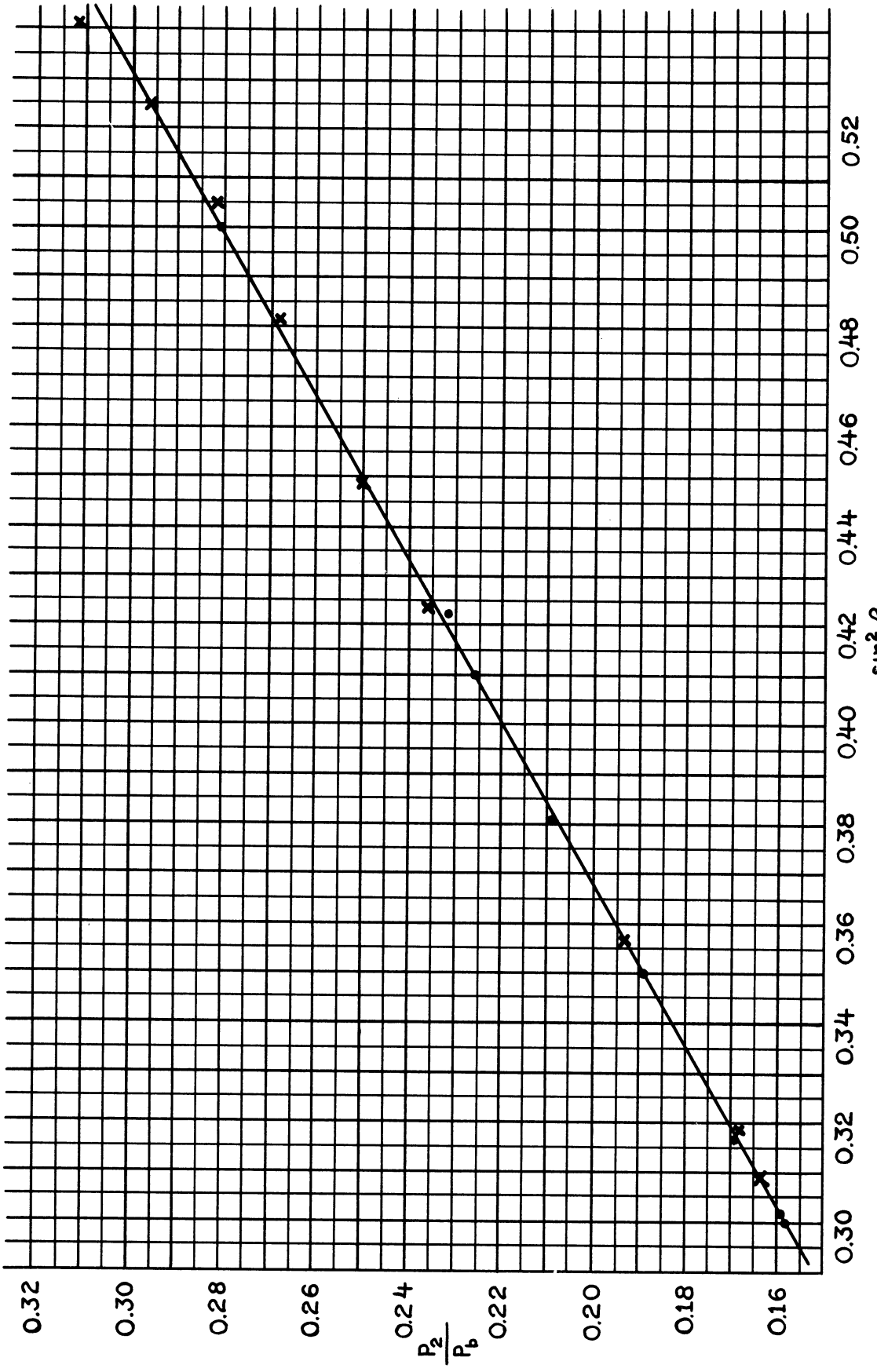

FIG. 13 – $\sin^2\beta$ VS $\frac{P_2}{P_b}$

From the data

$$\frac{4}{\gamma + 1}\left(\frac{q}{p_b}\right) = 0.617 \pm 0.004 \qquad (6)$$

$$\frac{q}{p_b} = 0.371 \pm 0.002$$

Thus from equation (4) the product

$$\left(\frac{p_1}{p_b}\right) M_1^2 = 0.527 \pm 0.003 \qquad (7)$$

is determined with considerable precision.

EXPERIMENTAL RESULTS

The ambient static pressure ratio as determined from the $p_2 = p_2(\theta)$ curve (Fig. 10) by the discontinuity in the $\beta = \beta(\theta)$ curve is

$$\frac{p_1}{p_b} = 0.1505 \pm 0.001$$

Using Equation (7) the Mach number is determined to be

$$M_1 = \sqrt{\frac{0.527}{0.1505}} = 1.872 \pm .006$$

The Mach number has also been determined directly by measuring the Mach or shock angle in three different ways:

1. From the weak oblique shock wave which is present in the tunnel when there is no model present (shown in Fig. 9) the shock angle, β , is 32.5°. The pressure ratio across this shock is approximately 1.016. The Mach number of the flow is then determined as approximately 1.87.

2. The Mach angle of the lines extending from the static probe were also determined. The Mach angle is 32.3° and the Mach number is correspondingly 1.872.

3. From the shock angle caused by a 20° cone, $\beta = 33.5^\circ$.

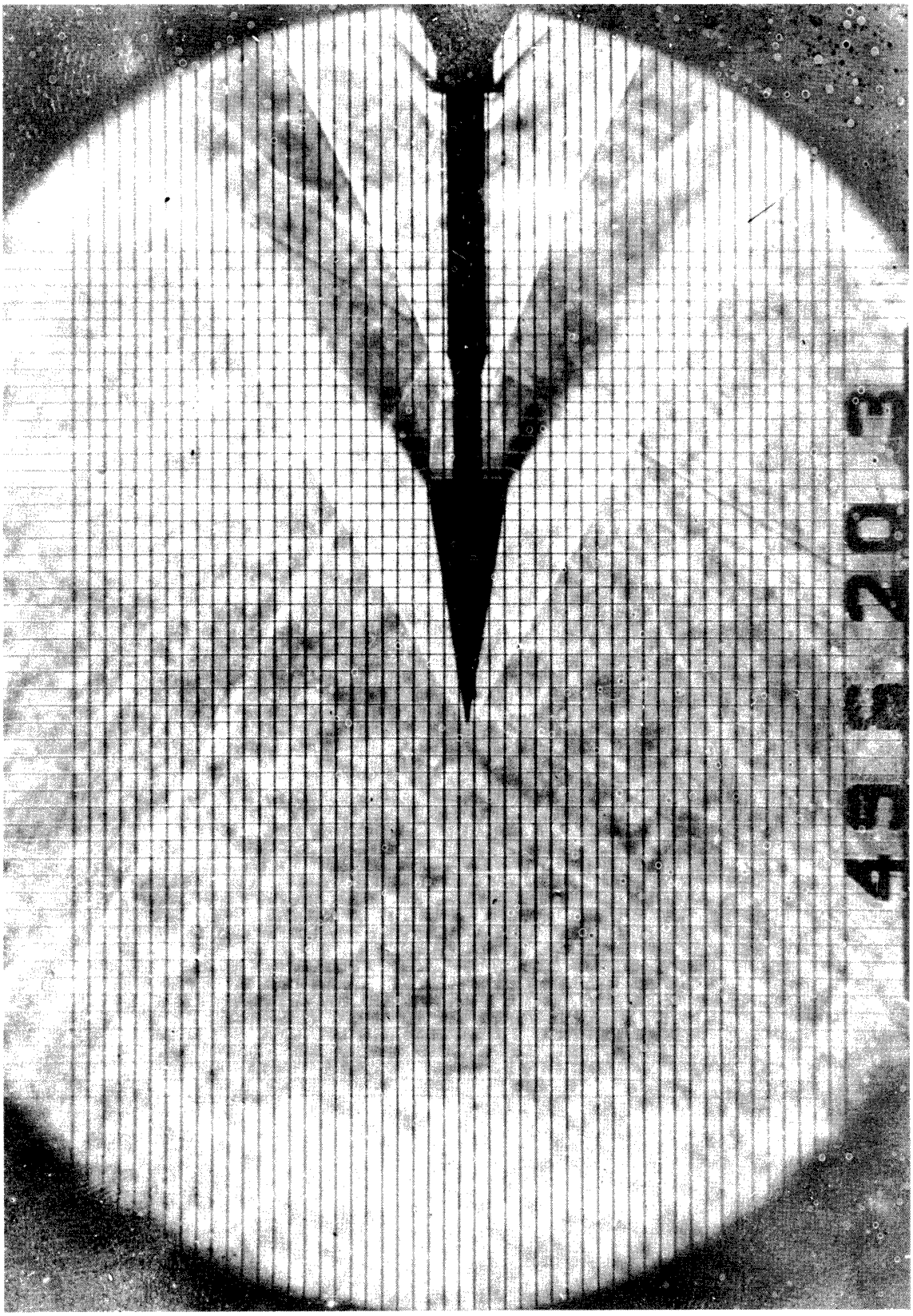

FIG. 14 — SCHLIEREN PHOTOGRAPH OF CONE MODEL

Allowing for a laminar boundary layer* the corresponding Mach number of the free stream is 1.873. The flow pattern is shown in figure 14.

The average of these values is taken as $M_1 = 1.873 \pm 0.005$. The higher value is chosen since the Mach angle measured from the static probe is actually a very weak shock line and hence should give a low value of M. The value from the cone should be more accurate.

The static pressure was also determined using the static probe shown in figure 15. This probe is a small cone-cylinder with the static orifice located 10 diameters from the forward end of the cylindrical portion. The values determined with this orifice range from 0.1482 to 0.1518 depending on the orientation of the angle of roll of the orifice position. These values are somewhat higher than those obtained from the previous calibration (Ref. 7 and 8). By use of a vacuum pump the absolute pressure reference was placed on the manometer board. All pressures were read directly from this reference. The values spread about the value of 0.1505 determined from the wedge method as shown in figure 10.

CHECK OF RESULTS

Using the values of M_1 and p_1/p_b as determined, the product

$$\left(\frac{p_1}{p_b}\right) \quad M_1^2$$

provides an excellent method of checking the results. The quantities $\frac{p_1}{p_b}$ and M_1 are each determined separately with accuracies as indicated. Then the value of the product is also measured separately and can be checked against the product calculated from the other two determinations. Thus the product becomes $(0.1505)\ (1.873)^2 = 0.528 \pm 0.002$. This is in good agreement with 0.527 ± 0.003 determined directly from equation (6).

The pressure, p_o', behind a normal shock was experimentally determined by a total head tube to be

$$\frac{p_o'}{p_b} = 0.760 \pm 0.002$$

*See footnote page 25

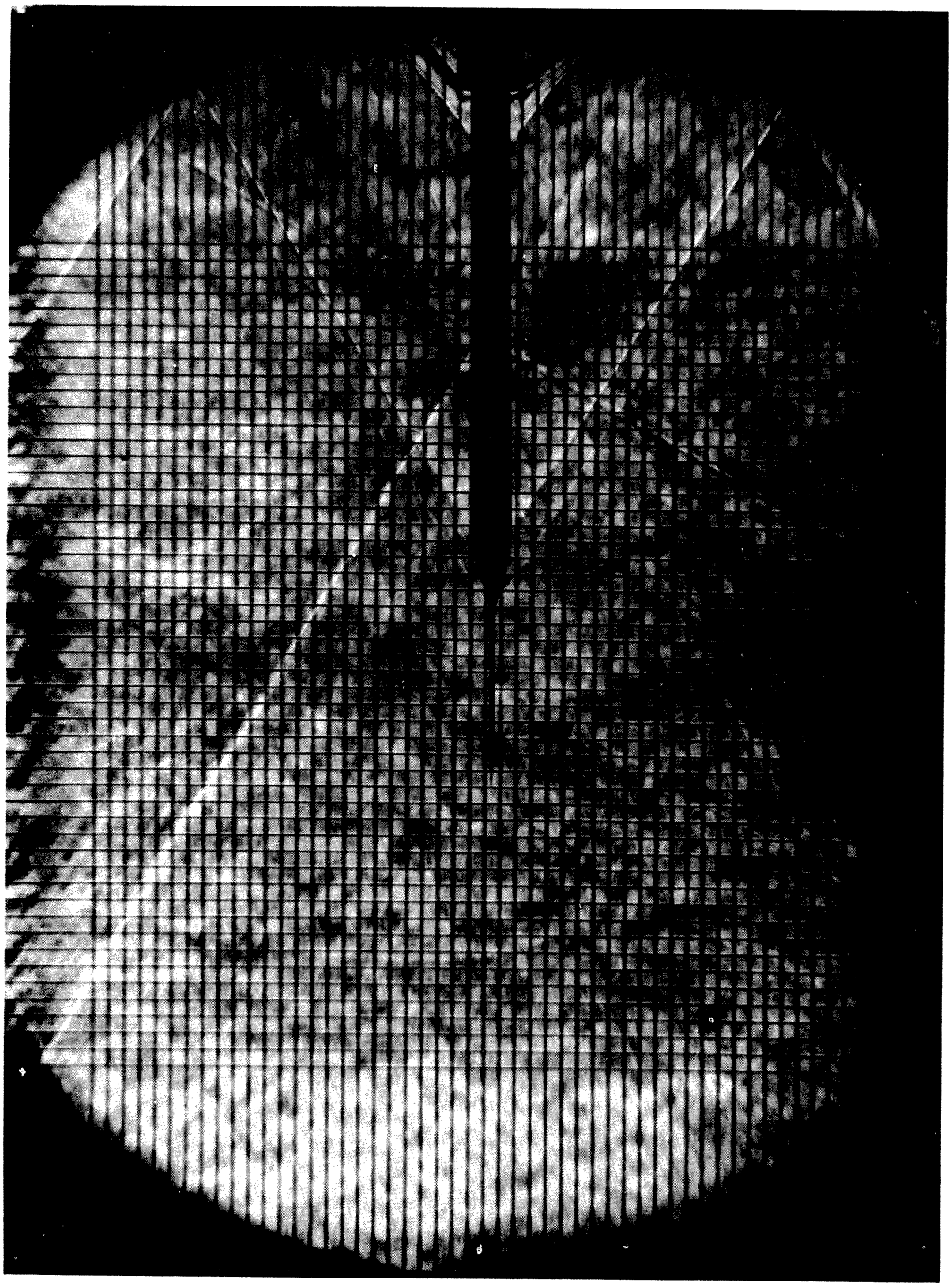

FIG. 15 – SCHLIEREN PHOTOGRAPH OF STATIC PROBE

For M = 1.873 the theoretical ratio to stagnation pressure, p_o, is

$$\frac{p_o'}{p_o} = 0.7798$$

Hence

$$\frac{p_o}{p_b} = \frac{0.760}{0.7798} = 0.975 \pm 0.004$$

p_o may also be determined as follows:

For M = 1.873, the theoretical ratio is

$$\frac{p_1}{p_o} = 0.1555$$

Hence

$$\frac{p_o}{p_b} = \frac{0.1505}{0.1555} = 0.968 \pm 0.006$$

These two values agree within limits of accuracy estimated and both indicate that the value of p_o is definitely less than the barometric pressure. Hence the flow along the tunnel center line outside the boundary layer is not strictly isentropic and any assumption to the contrary appears unjustified.

APPLICATION OF RESULTS

Using these calibration results which are summarized as follows:

$$\frac{p_1}{p_b} = 0.1505 \pm 0.001$$

$$M_1 = 1.873 \pm 0.006$$

$$\frac{q}{p_b} = 0.371 \pm 0.002$$

the pressure coefficients over the wedge, cone, and cone-cylinder are

determined as shown in figures 4, 10, and 16.
The following are noted:

1. For the wedge the close agreement of the experimental data to that of the theoretical curve calculated for M = 1.87, including boundary layer correction*, is evident from figure 10.

2. For the cone the comparison of data as given in figure 16 shows that the experimental data agrees with the theoretical value after allowance for boundary layer* within the limits of experimental scatter. The mean value of the experimental points agrees within 2%.

3. The corrected data for the cone-cylinder shown in figure 4 indicates closer correlation to the extrapolated value for the non-linear theory. In particular, the pressures near the aft end which were positive according to the previous calibration are now seen to be negative and are asymptotically approaching zero as predicted by theory.

---

* The boundary layer correction was calculated from

$$\delta^* = \frac{1.73x}{R}$$

Where δ^* is the boundary layer displacement thickness, x is the distance from the leading edge to the pressure orifice and R is the Reynolds number of the flow. The average angular increment $\Delta\theta$ where $\tan\theta = y/x$ was calculated from $\tan(\theta + \Delta\theta) = (y + \delta^*)/x$.

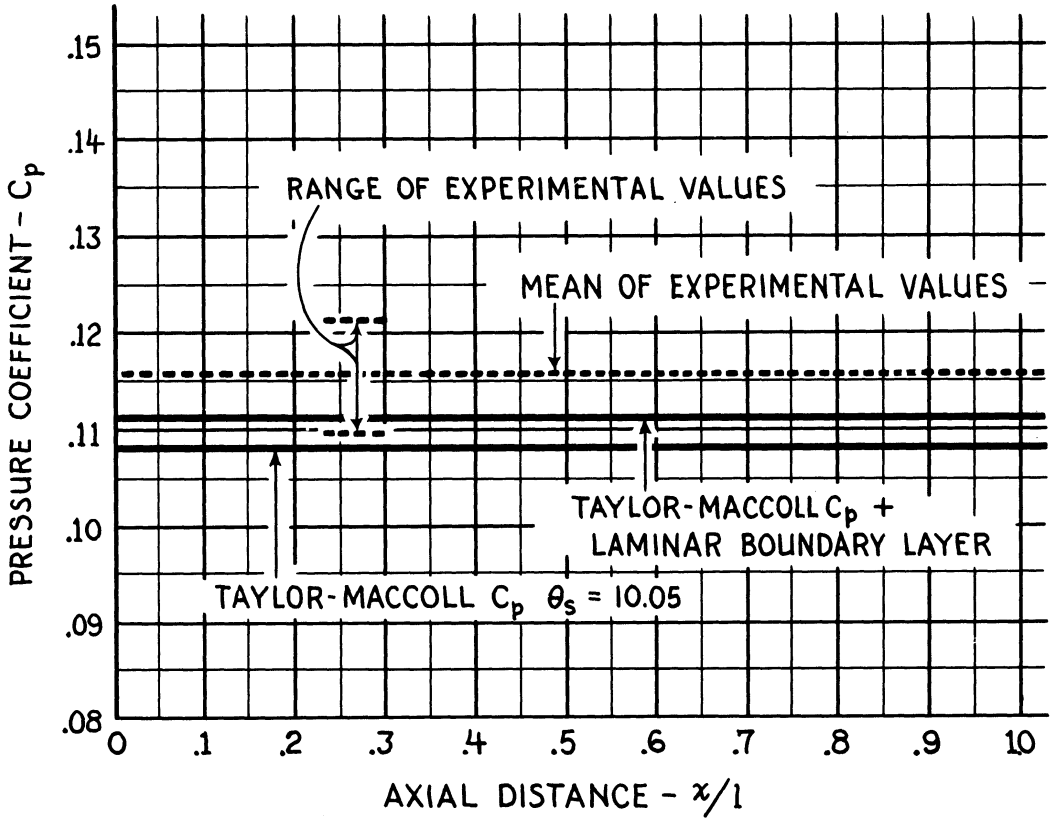

FIG. 16 — COMPARISON OF THEORETICAL AND EXPERIMENTAL DATA FOR 20° CONE, α = 0

CONCLUSION

The use of a wedge and non-linear oblique shock wave theory have been made to determine the ambient static pressure and Mach number in a supersonic stream. This method provides an excellent check for the results and gives an insight so that errors can be detected more readily. The procedure is independent of any assumptions about stagnation pressure, which can be calculated from data obtained in the other determinations.

The close correlation between theory and experiment which is obtained for pressures on a wedge, cone and cone-cylinder and for the corresponding shock wave angles, is cited as evidence of the accuracy of the method.

REFERENCES

1. Air Pressure on a Cone Moving at High Speeds, by G. I. Taylor and J. W. Maccoll, Royal Society, October 1932.

2. Pressure Survey on Cones in the Two-Dimensional, by I. D. Berkley, 1.75 M, Free Jet at F.G.S., Applied Physics Laboratory, Johns Hopkins University, CF-716.

3. Experimental Determination of Pressure on the Surface of a Cone in a Supersonic Stream, by I. D. Berkley, JHU/APL/CF-530.

4. Status Report on the Calibration of Wind Tunnel Nozzle, by R. Jackson. Unpublished report, Lone Star Laboratory, Daingerfield, Texas, 16 June 1947.

5. An Evaluation of the Discrepancy between Experiment and Theory for a Typical Pressure Distribution Test at a Mach No. of 1.93, by W. H. Dorrance, University of Michigan EMB-8, 29 November 1948.

6. The Experimental and Thoretical Pressure Distribution and Normal Force of a Cone-Cylinder Configuration at a Mach No. of 1.93, by W. H. Dorrance, University of Michigan EMB-10, 20 January 1949.

7. Final Calibration Report on the Mach 2 Configuration, Excluding Balance System in the U.M.E.R.I. Supersonic Wind Tunnel, by W. H. Curry, University of Michigan WTM-45, 20 September 1948.

8. Calibration of the U.M.E.R.I. Supersonic Wind Tunnel, by P. E. Culbertson, University of Michigan WTM-89, 27 May 1949.